SIAM J. SCI. COMPUT.
Vol. 42, No. 1, pp. A371–A394

TWO-SIDE A POSTERIORI ERROR ESTIMATES FOR THE DUAL-WEIGHTED RESIDUAL METHOD*

B. ENDTMAYER†, U. LANGER†, AND T. WICK‡

Abstract. In this work, we derive two-sided a posteriori error estimates for the dual-weighted residual (DWR) method. We consider both single and multiple goal functionals. Using a saturation assumption, we derive lower bounds yielding the efficiency of the error estimator. These results hold true for both nonlinear partial differential equations and nonlinear functionals of interest. Furthermore, the DWR method employed in this work accounts for balancing the discretization error with the nonlinear iteration error. We also perform careful studies of the remainder term that is usually neglected. Based on these theoretical investigations, several algorithms are designed. Our theoretical findings and algorithmic developments are substantiated with some numerical tests. Specifically, we also provide a counterexample in which the saturation assumption is violated.

Key words. dual-weighted residual method, multiple goal functionals, saturation assumption, efficiency and reliability of the error estimator, p-Laplacian, incompressible Navier–Stokes equations

AMS subject classifications. 65N30, 65M60, 65J15, 49M15, 35Q74

DOI. 10.1137/18M1227275

1. Introduction.

In many applications, nonlinear partial differential equations (PDEs) must be solved. Examples can be found in fluid mechanics, fluid structure interaction, solid mechanics, porous media, fracture/damage mechanics, and electromechanics. Specifically, in recent years, multiphysics problems in which several phenomena interact have become quite important due to the advancements of computational resources (in particular parallel computing and local mesh adaptivity). However, we are often interested not in the entire solution but in certain functionals of interest, also called goal functionals. Due to the nature of multiphysics problems, several goal functionals may be of interest simultaneously. Motivated by this fact, basic frameworks for the adaptive treatment of multiple goal functionals were first proposed in [42, 41]. Recently, other efforts have been undertaken in [59, 5, 47, 74, 31, 29, 30].

In these studies, adaptivity is based on a posteriori error estimation, which is a widely used and well developed tool in finite element method (FEM) computations as, for example, presented in [9, 12, 77, 8, 56, 3, 75, 68, 40, 33], and in other discretization techniques too; see, e.g., [7, 60, 49, 52, 72, 76].

The previously mentioned applications are too complicated for the rigorous numerical analysis that we have in mind. For this reason, we concentrate on the development of a posteriori error estimation for a prototype nonlinear stationary setting in this work. Here, we focus on both fundamental theoretical and practical aspects. Our method of choice is goal-oriented error estimation using the dual-weighted residual

*Submitted to the journal's Methods and Algorithms for Scientific Computing section November 16, 2018; accepted for publication (in revised form) October 18, 2019; published electronically February 19, 2020.
https://doi.org/10.1137/18M1227275
Funding: This work was supported by the Austrian Science Fund (FWF) under grant P 29181. The work of the third author was supported by RICAM.
†Johann Radon Institute for Computational and Applied Mathematics, Austrian Academy of Sciences, Altenbergerstr. 69, A-4040 Linz, Austria (bernhard.endtmayer@ricam.oeaw.ac.at, ulanger@numa.uni-linz.ac.at).
‡Leibniz Universität Hannover, Institut für Angewandte Mathematik, AG Wissenschaftliches Rechnen, Welfengarten 1, 30167 Hannover, Germany (thomas.wick@ifam.uni-hannover.de).

(DWR) method [19, 15, 65, 63, 17], which has proven to be a successful technique. In particular, we are interested in the quality of the error estimator. Furthermore, it would be desirable to obtain convergence rates for the corresponding adaptive procedure. Such convergence results are discussed in [54, 35, 45, 46]. Improvements of convergence rates are discussed in [61, 38, 62, 71]. Concerning upper bounds of the error, we mention the works [64, 57, 35, 4], where [64] also provides a lower bound for the energy norm in the case of linear symmetric elliptic boundary value problems, and [57] for a pointwise error estimate in case of monotone semilinear problems.

The first goal of this work is to prove upper and lower bounds for both nonlinear PDEs and nonlinear quantities of interest. This is done for a hierarchical approximation in the DWR error estimator. Hierarchical approaches for the DWR method are also used in [10, 42, 41, 69, 22, 50] exploiting higher-order elements. In this work, we use a partition of unity localization, which was developed in [69]. Here backward-integration by parts is not required. We can employ the variational form of the error estimator. Recently, this localization was also applied to other discretization techniques like the finite cell method [72] or BEM-based FEM on polygonal meshes [76].

To prove the upper and lower bounds for our error estimator, we need a saturation assumption for the quantity of interest. For other hierarchical-based a posteriori error estimates in the energy norm, this is a widely used assumption [13, 20, 12, 75], where [20] proved that the saturation assumption can be violated preasymptotically for certain data. For some elliptic boundary value problems, the saturation assumption is proven in the energy norm for small data oscillations; see, e.g., [28, 36, 23] and [11] for hp-FEM and [2, 1] for a modified version of this assumption. Furthermore, a proof of the saturation assumption for a convection-diffusion problem in one dimension is derived in [25, 48]. However, we are not aware of results for general goal functionals. We notice that this is even infeasible because the functional error can be zero for general goal functionals. Therefore, a positive lower bound cannot be obtained. A step in this direction was achieved in [69], where a common bound for the functional error and the error indicators could be established for several often employed localization techniques.

We emphasize that our previous developments apply to the generalized version of the DWR method in which not only is the discretization error is addressed, but also the iteration error can be balanced with the discretization error [16, 34, 53, 66, 67]. In particular, following [66], in our previous work [29], we developed and extended such a framework that applies to single and multiple goal functionals. We notice that, in contrast to these works, we represent the iteration error in the current paper in a different way, which avoids the solution of the adjoint problem for checking the adaptive stopping criterion of Newton's method. This stopping criteria of Newton's method is also affine-invariant and falls consequently into the category of Newton schemes discussed in [26].

The second goal of this work consists in the investigation of the several parts of the DWR error estimator. More precisely, we consider both single and multiple goal functionals, both the primal and adjoint parts, the iteration error estimator, and the nonlinear remainder part. In particular, the latter term is often neglected in the literature.

The outline of this paper is as follows. In section 2, we introduce the abstract setting and briefly recap the basic concept of the DWR method. Section 3 contains our main result. Under a saturation assumption, we first prove lower and upper bounds for a computable error estimator. Then, using a slightly strengthened version, we establish bounds for the practicable error estimator. The different parts of the error estimator and their localization are discussed in section 4, followed by a discussion for multiple goal functionals in section 5. In this discussion, we derive sufficient conditions to avoid error cancellation under our saturation assumption. The resulting algorithms are presented in detail in section 6 for the finite element method. In principle, they can also be easily applied to other discretization techniques like isogeometric analysis, finite volume methods, finite cell methods, or virtual element methods. Section 7 provides the results of our numerical experiments. We performed extensive numerical tests for both single goal and multiple goal functional evaluations at finite element solutions of the regularized p-Laplace equation; see also [27, 44, 73]. Then, in section 7.2, a counterexample is presented in which the saturation assumption is not fulfilled. Finally, our observations are summarized in section 8.

2. The dual weighted residual method for nonlinear problems.

In this section, we briefly recall the abstract setting of our previous work [29].

2.1. An abstract setting.

Let U and V be Banach spaces, and let $\mathcal{A}: U \mapsto V^*$ be a nonlinear operator, where V^* denotes the dual space of the Banach space V. We consider the primal problem: Find $u \in U$ such that

$$\mathcal{A}(u) = 0 \qquad \text{in } V^*. \tag{2.1}$$

Furthermore, we consider finite dimensional subspaces $U_h \subset U$ and $V_h \subset V$. In this paper, U_h and V_h are finite element spaces (we notice, however, that our ideas are not restricted to a particular discretization method). This leads to the following finite dimensional problem: Find $u_h \in U_h$ such that

$$\mathcal{A}(u_h) = 0 \qquad \text{in } V_h^*. \tag{2.2}$$

We assume that both (2.1) and (2.2) are solvable. Further assumptions will be imposed later.

However, we are not primarily interested in a solution of (2.1) itself, but in one or even several functional evaluations, so-called goal functionals, evaluated at $u \in U$ and $u_h \in U_h$, and their resulting distance, respectively.

2.2. The dual weighted residual method.

We now recall the DWR method for nonlinear problems [19]. The extensions for balancing the discretization and iteration errors were undertaken in [66, 67, 53]. In particular, we base our work on [66], where iteration errors of the nonlinear solver were considered. This paper forms together with our previous works [69, 31, 29, 30] the basis of the current study. To apply the DWR method, we have to consider the adjoint problem: Find $z \in V$ such that

$$\left(\mathcal{A}'(u)\right)^* (z) = J'(u) \qquad \text{in } U^*, \tag{2.3}$$

where $\mathcal{A}'(u)$ and $J'(u)$ denote the Fréchet derivatives of the nonlinear operator and functional, respectively, evaluated at u. Later we will also need the finite dimensional version of (2.3) that reads as follows: Find $z_h \in V_h$ such that

$$\left(\mathcal{A}'(u_h)\right)^* (z_h) = J'(u_h) \qquad \text{in } U_h^*. \tag{2.4}$$

Similarly to the findings in [66, 19, 67] for the Galerkin case ($U = V$), we provide an error representation in the following theorem.

THEOREM 2.1. *Let us assume that* $\mathcal{A} \in \mathcal{C}^3(U,V)$ *and* $J \in \mathcal{C}^3(U,\mathbb{R})$*. If* u *solves* (2.1) *and* z *solves* (2.3) *for* $u \in U$*, then the error representation*

$$J(u) - J(\tilde{u}) = \frac{1}{2}\rho(\tilde{u})(z-\tilde{z}) + \frac{1}{2}\rho^*(\tilde{u},\tilde{z})(u-\tilde{u}) + \rho(\tilde{u})(\tilde{z}) + \mathcal{R}^{(3)}$$

holds true for arbitrary fixed $\tilde{u} \in U$ *and* $\tilde{z} \in V$*, where* $\rho(\tilde{u})(\cdot) := -\mathcal{A}(\tilde{u})(\cdot)$*,* $\rho^*(\tilde{u},\tilde{z})(\cdot) := J'(u) - \mathcal{A}'(\tilde{u})(\cdot,\tilde{z})$*, and the remainder term*

$$\begin{aligned}\mathcal{R}^{(3)} := \frac{1}{2}\int_0^1 &[J'''(\tilde{u}+se)(e,e,e) - \mathcal{A}'''(\tilde{u}+se)(e,e,e,\tilde{z}+se^*) \\ &- 3\mathcal{A}''(\tilde{u}+se)(e,e,e)]s(s-1)\,ds,\end{aligned} \tag{2.5}$$

with $e = u - \tilde{u}$ *and* $e^* = z - \tilde{z}$*.*

Proof. We refer the reader to [29] and [66] for the details of the proof. ∎

Since Theorem 2.1 is valid for arbitrary $\tilde{z}$ and $\tilde{u}$, it also holds for the approximations u_h and z_h, even if they are not computed exactly. Thus, the full error estimator reads as

$$\eta = \frac{1}{2}\rho(\tilde{u})(z-\tilde{z}) + \frac{1}{2}\rho^*(\tilde{u},\tilde{z})(u-\tilde{u}) + \rho(\tilde{u})(\tilde{z}) + \mathcal{R}^{(3)}. \tag{2.6}$$

This error estimator is exact, however, not computable. To obtain a computable error estimator, we replace u by an approximation on enriched finite dimensional spaces $U_h^{(2)}$ and $V_h^{(2)}$, which, for example, was also done in [38, 10, 22, 50, 69, 31, 29, 30]. In our numerical examples presented in section 7, we use bi-quadratic (two-dimensional (2D)) finite elements to define the enriched spaces $U_h^{(2)}$ and $V_h^{(2)}$. As in [31], spaces with polynomial orders $r > 2$ can be adopted as well.

Remark 1. Using enriched spaces is expensive. For this reason, in the early studies, e.g., [19, 10, 21], (patchwise) interpolations were suggested to approximate z and u.

3. Efficiency and reliability results for the DWR estimator. In this key section, we show efficiency and reliability of a computable DWR estimator in enriched spaces under a saturation assumption for the goal functional. As mentioned in the introduction, this is a widely adopted assumption in hierarchical-based error estimates; see, e.g., [13, 20, 12, 75]. We are not aware of literature satisfying this assumption for general nonlinear problems and goal functionals. Furthermore, there might be restrictions to satisfy this condition. For error estimates in the energy norm, an analysis regarding this assumption can be found in [28, 2, 1, 36, 11, 23, 32] for linear elliptic boundary value problems depending on the oscillation of the data. Finally, we employ higher-order corrections of the error estimator. Similar ideas correcting the functional value were discussed in [38, 37, 71]. Such techniques have also been used to derive an upper bound of the error without using the saturation assumption in [58, 4, 51]. Lower and upper bounds were established for symmetric linear elliptic boundary value problems in [64] and for monotone and semilinear problems for pointwise error estimates in [57].

3.1. Preliminary results. We now first recall some notation and known statements. Let $u_h^{(2)} \in U_h^{(2)}$ be the exact solution of the discretized primal problem $\mathcal{A}(u_h^{(2)}) = 0$ in $(V_h^{(2)})^*$, and $z_h^{(2)} \in V_h^{(2)}$ the exact solution of the discretized adjoint problem $(\mathcal{A}'(u_h^{(2)}))^*(z_h^{(2)}) = J'(u_h^{(2)})$ in $(U_h^{(2)})^*$.

COROLLARY 3.1. *Let the assumptions of Theorem* 2.1 *be fulfilled. Then the error representation*

$$J(u_h^{(2)}) - J(\tilde{u}) = \frac{1}{2}\rho(\tilde{u})(z_h^{(2)} - \tilde{z}) + \frac{1}{2}\rho^*(\tilde{u},\tilde{z})(u_h^{(2)} - \tilde{u}) + \rho(\tilde{u})(\tilde{z}) + \mathcal{R}^{(3)(2)}$$

holds for arbitrary but fixed $\tilde{u} \in U_h^{(2)}$ *and* $\tilde{z} \in V_h^{(2)}$*, where* $\rho(\tilde{u})(\cdot) := -\mathcal{A}(\tilde{u})(\cdot)$, $\rho^*(\tilde{u},\tilde{z})(\cdot) := J'(\tilde{u}) - \mathcal{A}'(\tilde{u})(\cdot,\tilde{z})$*, and* $\mathcal{R}^{(3)(2)} := \frac{1}{2}\int_0^1 [J'''(\tilde{u}+se^{(2)})(e^{(2)},e^{(2)},e^{(2)}) - \mathcal{A}'''(\tilde{u}+se^{(2)})(e^{(2)},e^{(2)},e^{(2)},\tilde{z}+se^{(2),*}) - 3\mathcal{A}''(\tilde{u}+se^{(2)})(e^{(2)},e^{(2)},e^{(2),*})]s(s-1)\,ds$ *denotes the remainder term, with* $e^{(2)} = u_h^{(2)} - \tilde{u}$ *and* $e^{(2),*} = z_h^{(2)} - \tilde{z}$.

Proof. The statement follows immediately from Theorem 2.1. ∎

Remark 2. For a linear problem and a functional fulfilling $J''' = 0$ this theorem allows us to compute $J(u_h^{(2)})$ without the computation of $u_h^{(2)}$ since $\rho(\tilde{u})(z_h^{(2)} - \tilde{z}) = \rho^*(\tilde{u},\tilde{z})(u_h^{(2)} - \tilde{u})$ for linear problems as already stated in [38].

Replacing u and z by the approximations $u_h^{(2)}$ and $z_h^{(2)}$ in (2.6), we get the computable error estimator

$$\eta^{(2)} := \frac{1}{2}\rho(\tilde{u})(z_h^{(2)} - \tilde{z}) + \frac{1}{2}\rho^*(\tilde{u},\tilde{z})(u_h^{(2)} - \tilde{u}) + \rho(\tilde{u})(\tilde{z}) + \mathcal{R}^{(3)(2)}. \tag{3.1}$$

Now, Corollary 3.1 together with (3.1) allows us to recover the error $J(u_h^{(2)}) - J(\tilde{u})$. A similar representation of the error $J(u_h^{(2)}) - J(\tilde{u})$ is derived in [38, 37, 62].

3.2. Efficiency and reliability of the DWR estimator using a saturation assumption. The following lemma provides a two-side estimate of the modulus of $\eta^{(2)}$ defined by (3.1).

LEMMA 3.2. *Under the assumptions of Theorem* 2.1, *the two-side estimate*

$$|J(u) - J(\tilde{u})| - |J(u) - J(u_h^{(2)})| \le |\eta^{(2)}| \le |J(u) - J(\tilde{u})| + |J(u) - J(u_h^{(2)})|$$

holds for the computable error estimator $\eta^{(2)}$.

Proof. From $|\eta| = |\eta^{(2)} - (\eta^{(2)} - \eta)|$, we can deduce that

$$|\eta| - |\eta - \eta^{(2)}| \le |\eta^{(2)}| \le |\eta| + |\eta - \eta^{(2)}|.$$

Since $U_h^{(2)}$ is an enriched space, we have $U_h \subset U_h^{(2)} \subset U$. It follows that $\eta - \eta^{(2)} = J(u) - J(\tilde{u}) - J(u_h^{(2)}) + J(\tilde{u}) = J(u) - J(u_h^{(2)})$, which leads us together with $\eta = J(u) - J(\tilde{u})$ to the estimates stated in the lemma. ∎

Assumption 1 (saturation assumption for the goal functional). Let $u_h^{(2)}$ solve the primal problem on $U_h^{(2)}$ and let $\tilde{u}$ be some approximation. Then we assume that

$$|J(u) - J(u_h^{(2)})| < b_h|J(u) - J(\tilde{u})|$$

for some $b_h < b_0$ and some fixed $b_0 \in (0,1)$.

THEOREM 3.3. *Let the saturation assumption, Assumption* 1*, be fulfilled. Then the computable error estimator* $\eta^{(2)}$ *satisfies the efficiency and reliability estimates*

$$\underline{c}_h|\eta^{(2)}| \le |J(u) - J(\tilde{u})| \le \overline{c}_h|\eta^{(2)}| \quad \text{and} \quad \underline{c}|\eta^{(2)}| \le |J(u) - J(\tilde{u})| \le \overline{c}|\eta^{(2)}| \tag{3.2}$$

with the positive constants $\underline{c}_h := 1/(1+b_h)$, $\overline{c}_h := 1/(1-b_h)$, $\underline{c} := 1/(1+b_0)$*, and* $\overline{c} := 1/(1-b_0)$.

Proof. In the proof of Lemma 3.2, we concluded that $|\eta| - |\eta - \eta^{(2)}| \leq |\eta^{(2)}| \leq |\eta| + |\eta - \eta^{(2)}|$, which is equivalent to the statement that $|\eta^{(2)}| - |\eta^{(2)} - \eta| \leq |\eta| \leq |\eta^{(2)}| + |\eta^{(2)} - \eta|$. Therefore, we have

$$|\eta^{(2)}| - |J(u) - J(u_h^{(2)})| \leq |J(u) - J(\tilde{u})| \leq |\eta^{(2)}| + |J(u) - J(u_h^{(2)})|,$$

which together with Assumption 1 immediately yields the first inequalities in (3.2). The second statement follows from $\underline{c} \leq \underline{c}_h$ and $\overline{c}_h \leq \overline{c}$ due to $b_h < b_0$. ∎

Remark 3. The left estimate in (3.2) also holds for $b_0 \in (0, 1]$, which is called the weak saturation assumption in the case of energy norm estimates; see [23].

Now let us assume that we neglect the remainder term $\mathcal{R}^{(3)(2)}$ and iteration error estimator $\rho(\tilde{u})(\tilde{z})$ in the error estimator $\eta^{(2)}$. This gives the practical error estimator

$$\eta_h^{(2)} := \frac{1}{2}\rho(\tilde{u})(z_h^{(2)} - \tilde{z}) + \frac{1}{2}\rho^*(\tilde{u}, \tilde{z})(u_h^{(2)} - \tilde{u}), \tag{3.3}$$

where the corresponding theoretical error estimator is given by

$$\eta_h := \frac{1}{2}\rho(\tilde{u})(z - \tilde{z}) + \frac{1}{2}\rho^*(\tilde{u}, \tilde{z})(u - \tilde{u}). \tag{3.4}$$

Variants of these error estimators are discussed, e.g., in [19, 66, 69]; also see the references therein.

LEMMA 3.4. *Let η_h be defined as in* (3.4) *and $\eta_h^{(2)}$ be defined as in* (3.3). *Furthermore, let us assume that the assumptions of Theorem* 2.1 *are fulfilled. Then, for the exact solutions $u_h^{(2)}$ and $z_h^{(2)}$ from the spaces $U_h^{(2)}$ and $V_h^{(2)}$, the two-side estimates*

$$|J(u) - J(u_h^{(2)})| - |\mathcal{R}^{(3)} - \mathcal{R}^{(3)(2)}| \leq |\eta_h - \eta_h^{(2)}| \leq |J(u) - J(u_h^{(2)})| + |\mathcal{R}^{(3)} - \mathcal{R}^{(3)(2)}| \tag{3.5}$$

and

$$|J(u) - J(\tilde{u})| - |\rho(\tilde{u})(\tilde{z})| - |\mathcal{R}^{(3)}| \leq |\eta_h| \leq |J(u) - J(\tilde{u})| + |\rho(\tilde{u})(\tilde{z})| + |\mathcal{R}^{(3)}| \tag{3.6}$$

hold, with $\mathcal{R}^{(3)}$ defined in (2.5) *and $\mathcal{R}^{(3)(2)}$ from Corollary* 3.1.

Proof. From Theorem 2.1, we know that

$$J(u) - J(\tilde{u}) = \underbrace{\frac{1}{2}\rho(\tilde{u})(z - \tilde{z}) + \frac{1}{2}\rho^*(\tilde{u}, \tilde{z})(u - \tilde{u})}_{\eta_h} + \rho(\tilde{u})(\tilde{z}) + \mathcal{R}^{(3)},$$

and Corollary 3.1 provides us with the identity

$$J(u_h^{(2)}) - J(\tilde{u}) = \underbrace{\frac{1}{2}\rho(\tilde{u})(z_h^{(2)} - \tilde{z}) + \frac{1}{2}\rho^*(\tilde{u}, \tilde{z})(u_h^{(2)} - \tilde{u})}_{\eta_h^{(2)}} + \rho(\tilde{u})(\tilde{z}) + \mathcal{R}^{(3)(2)}.$$

These two identities imply the identity $J(u) - J(u_h^{(2)}) = \eta_h - \eta_h^{(2)} + \mathcal{R}^{(3)} - \mathcal{R}^{(3)(2)}$. We now conclude that $|J(u) - J(u_h^{(2)}) - \mathcal{R}^{(3)} + \mathcal{R}^{(3)(2)}| = |\eta_h - \eta_h^{(2)}|$, from which we immediately get the inequalities (3.5). The second statement follows directly from Theorem 2.1. ∎

LEMMA 3.5. *Under the conditions of Lemma* 3.4, *inequalities*

$$|\eta_h^{(2)}| - \gamma(\mathcal{A}, J, u_h^{(2)}, u, \tilde{u}) \leq |J(u) - J(\tilde{u})| \leq |\eta_h^{(2)}| + \gamma(\mathcal{A}, J, u_h^{(2)}, u, \tilde{u}) \tag{3.7}$$

are valid, where

$$\gamma(\mathcal{A}, J, u_h^{(2)}, u, \tilde{u}) := |J(u) - J(u_h^{(2)})| + |\mathcal{R}^{(3)} - \mathcal{R}^{(3)(2)}| + |\rho(\tilde{u})(\tilde{z})| + |\mathcal{R}^{(3)}|. \tag{3.8}$$

Proof. Inequalities (3.7) immediately follow from (3.5), (3.6), and

$$|\eta_h| - |\eta_h - \eta_h^{(2)}| \leq |\eta_h^{(2)}| \leq |\eta_h| + |\eta_h - \eta_h^{(2)}|. \qquad \square$$

3.3. Practicable error estimator under a strengthened saturation assumption. We refine our previous analysis in order to derive a similar statement for the practicable error estimator $\eta_h^{(2)}$. We suppose the following strengthened saturation assumption.

Assumption 2 (strengthened saturation assumption for the goal functional). Let $u_h^{(2)}$ solve the primal problem on $U_h^{(2)}$, and let $\tilde{u}$ be some approximation. Then we assume that the inequality

$$\gamma(\mathcal{A}, J, u_h^{(2)}, u, \tilde{u}) < b_{h,\gamma}|, J(u) - J(\tilde{u})|,$$

with $\gamma(\cdot)$ defined in (3.8), holds true for some $b_{h,\gamma} < b_{0,\gamma}$ with some fixed $b_{0,\gamma} \in (0, 1)$.

Remark 4. Of course, Assumption 2 implies Assumption 1. If, on the other hand, Assumption 1 holds, then Assumption 2 is fulfilled up to higher-order terms ($|\mathcal{R}^{(3)} - \mathcal{R}^{(3)(2)}|$, $|\mathcal{R}^{(3)}|$), and the part $|\rho(\tilde{u})(\tilde{z})|$, which can be controlled by the accuracy of the nonlinear solver.

THEOREM 3.6. *Let the saturation assumption, Assumption* 2, *be fulfilled. Then the practical error estimator $\eta_h^{(2)}$ satisfies the efficiency and reliability estimates*

$$\underline{c}_{h,\gamma}|\eta_h^{(2)}| \leq |J(u) - J(\tilde{u})| \leq \overline{c}_{h,\gamma}|\eta_h^{(2)}| \quad \text{and} \quad \underline{c}_{\gamma}|\eta_h^{(2)}| \leq |J(u) - J(\tilde{u})| \leq \overline{c}_{\gamma}|\eta_h^{(2)}| \tag{3.9}$$

with the positive constants $\underline{c}_{h,\gamma} := 1/(1 + b_{h,\gamma})$, $\overline{c}_{h,\gamma} := 1/(1 - b_{h,\gamma})$, $\underline{c}_{\gamma} := 1/(1 + b_{0,\gamma})$, $\overline{c}_{\gamma} := 1/(1 - b_{0,\gamma})$.

Proof. From Lemma 3.5, we concluded that $|\eta_h^{(2)}| - \gamma(\mathcal{A}, J, u_h^{(2)}, u, \tilde{u}) \leq |J(u) - J(\tilde{u})| \leq |\eta_h^{(2)}| + \gamma(\mathcal{A}, J, u_h^{(2)}, u, \tilde{u})$, which together with Assumption 2 implies that

$$\frac{1}{1 + b_{h,\gamma}}|\eta_h^{(2)}| \leq |J(u) - J(\tilde{u})| \leq \frac{1}{1 - b_{h,\gamma}}|\eta_h^{(2)}|.$$

This is our first statement. Like in the proof of Theorem 3.3, the second statement follows from $\underline{c}_{\gamma} \leq \underline{c}_{h,\gamma}$ and $\overline{c}_{h,\gamma} \leq \overline{c}_{\gamma}$. We mention that $b_{h,\gamma} < b_{0,\gamma}$. $\square$

Remark 5. The left estimate in (3.9) is also true for $b_{0,\gamma} \in (0, 1]$.

3.4. Bounds of the effectivity indices. We finally derive bounds for the effectivity indices I_{eff} and $I_{eff,\gamma}$ defined by the relations

$$I_{eff} := \frac{|\eta^{(2)}|}{|J(u) - J(\tilde{u})|} \quad \text{and} \quad I_{eff,\gamma} := \frac{|\eta_h^{(2)}|}{|J(u) - J(\tilde{u})|},$$

respectively.

THEOREM 3.7 (bounds on the effectivity index). *Let the assumptions of Theorem 2.1 be fulfilled. Then the following two statements are true:*

1. *If Assumption 1 is fulfilled, then* $I_{eff} \in [1-b_0, 1+b_0]$*, and if additionally* $b_h \to 0$*, then* $I_{eff} \to 1$.
2. *If Assumption 2 is fulfilled, then* $I_{eff,\gamma} \in [1-b_{0,\gamma}, 1+b_{0,\gamma}]$*, and if additionally* $b_{h,\gamma} \to 0$*, then* $I_{eff,\gamma} \to 1$.

Proof. The first statement follows from Lemma 3.2 and Assumption 1, whereas the second statement is obtained from Lemma 3.5 and Assumption 2 in the same way. ∎

Remark 6. We notice that $I_{eff,\gamma} \to 1$ was also already observed in [10] and proven for smooth adjoint solutions in the linear case.

PROPOSITION 3.1. *If* $J''' \equiv 0$ *and if* A'' *is of the form* $A''(u) \equiv Bu + C$ *for some linear operator* B *and some* C *not depending on* u*, then we have the representation*

$$\mathcal{R}^{(3)} = \frac{1}{24}\left(3(B(u+\tilde{u}))(e,e,e^*) + (Be)(e,e,z+\tilde{z})\right) + \frac{1}{4}C(e,e,e^*).$$

Remark 7. In this section we did not consider the error contributions from the approximation of the data (source terms, boundary conditions) and quadrature formulas.

For later purposes, we finally define two additional effectivity indices:

$$I_{eff,p} := \frac{|\rho(\tilde{u})(z_h^{(2)} - z_h)|}{|J(u) - J(u_h)|}, \tag{3.10}$$

$$I_{eff,a} := \frac{|\rho^*(\tilde{u},\tilde{z})(u_h^{(2)} - u_h)|}{|J(u) - J(u_h)|}. \tag{3.11}$$

4. Localization and discussions of the error estimator parts.

In this section, we further discuss the computable error estimator $\eta^{(2)}$ defined in (3.1). We separate the error estimator $\eta^{(2)}$ into the following three parts $\eta_h^{(2)}$, η_k, and $\eta_{\mathcal{R}}^{(2)}$ as follows:

$$\eta^{(2)} := \underbrace{\frac{1}{2}\rho(\tilde{u})(z_h^{(2)} - \tilde{z}) + \frac{1}{2}\rho^*(\tilde{u},\tilde{z})(u_h^{(2)} - \tilde{u})}_{:=\eta_h^{(2)}} + \underbrace{\rho(\tilde{u})(\tilde{z})}_{:=\eta_k} + \underbrace{\mathcal{R}^{(3)(2)}}_{:=\eta_{\mathcal{R}}^{(2)}}.$$

The first part $\eta_h^{(2)}$ *of the error estimator* $\eta^{(2)}$. Following [66], we relate the discretization error to $\eta_h^{(2)}$. We use the partition of unity approach developed in [69] to localize $\eta_h^{(2)}$. This means that we choose a set of functions $\{\psi_1, \psi_2, \ldots, \psi_N\}$ (a typical choice would be the finite element basis functions) such that $\sum_{i=1}^N \psi_i \equiv 1$. Therefore, we have the representation

$$\eta_h^{(2)} := \sum_{i=1}^N \eta_i$$

with

$$\eta_i := \frac{1}{2}\rho(\tilde{u})((z_h^{(2)} - \tilde{z})\psi_i) + \frac{1}{2}\rho^*(\tilde{u},\tilde{z})((u_h^{(2)} - \tilde{u})\psi_i). \tag{4.1}$$

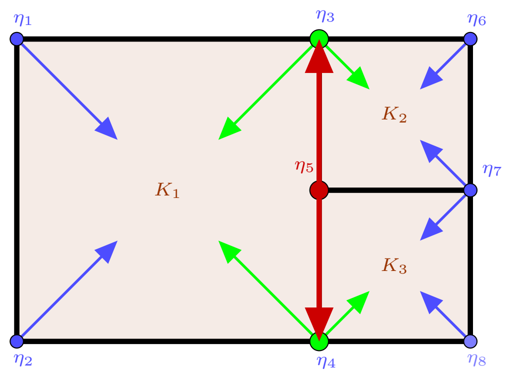

FIG. 1. *Distribution of the error contribution in a hanging node (red) to the neighboring nodes on the coarser element (green) for Q_c^1 basis functions as partition of unity.*

However, in contrast to our previous work [29], we emphasize that we do not replace $\tilde{z}$ by $i_h z_h^{(2)}$. In our numerical examples, we choose conforming bilinear elements Q_1^c for our partition of unity. Furthermore, we distribute the error contributions contained in hanging nodes in a way that is different from our previous work. For the partition of unity used in our numerical experiments, we distribute the error as in our previous work, however, splitting the error in the hanging nodes into two equal parts and adding the distribution to the neighboring nodes which belong to the coarse element, as illustrated in Figure 1.

The second part η_k of the error estimator $\eta^{(2)}$. The second part, $\eta_k = \rho(\tilde{u})(\tilde{z})$, is related to the iteration error as in [66]. Therefore, we can use this quantity as a stopping rule for the nonlinear solver, e.g., for Newton's method. In [29] and [66], $\tilde{z}$ was computed in every Newton step in order to evaluate the stopping criteria. If we further follow the path in [29] and compare the iteration error not to the current discretization error as in [66] but to the discretization error of the previous mesh, we can use the following lemma to reduce the computational cost.

LEMMA 4.1. *Let $\tilde{u}$ be an arbitrary element from U, and let $\delta\tilde{u} \in U$ be the solution of the problem, Find $\delta\tilde{u} \in U$ such that*

$$\mathcal{A}'(\tilde{u})(\delta\tilde{u}, v) = -\mathcal{A}(\tilde{u})(v) \qquad \forall v \in V, \tag{4.2}$$

and let $\hat{z} \in V$ be the solution of the problem, Find $\hat{z} \in V$ such that

$$\mathcal{A}'(\tilde{u})(v, \hat{z}) = J'(\tilde{u})(v) \qquad \forall v \in U. \tag{4.3}$$

Then we have the equation $-\mathcal{A}(\tilde{u})(\hat{z}) = J'(\tilde{u})(\delta\tilde{u})$.

Proof. It is trivial to see that $-\mathcal{A}(\tilde{u})(\hat{z}) = \mathcal{A}'(\tilde{u})(\delta\tilde{u}, \hat{z}) = J'(\tilde{u})(\delta\tilde{u})$. ∎

Remark 8. This means that instead of solving the adjoint problem, we can solve for the upcoming Newton updates in advance. This holds true only if the Newton updates $\delta\tilde{u}$ and $\hat{z}$ are the exact solutions of (4.3) and (4.2), respectively.

The third part $\eta_{\mathcal{R}}^{(2)}$ of the error estimator $\eta^{(2)}$. The third part, $R^{(3)(2)}$, was neglected in [29]. We localize this error by the local contributions of this error estimator parts computed on the elements. This leads to the local remainder

$$\eta_{\mathcal{R},K}^{(2)} := \mathcal{R}_{|K}^{(3)(2)} \tag{4.4}$$

in the third error estimator part on the element K. Alternatively, one could also use again the partition of unity approach, which was discussed for the first part.

5. Multiple goal functionals. For completeness of presentation we briefly recall the multigoal approach presented in [29]. From a general point of view, it may be questionable whether this approach is computationally interesting in comparison to the use of uniform mesh refinement. However, our previous studies have shown excellent results. Moreover, this approach has the advantage that we have an error estimator (and not only indicators for mesh refinement) providing us concrete quantitative numbers that are useful as stopping criteria for iterative solvers or error information about quantities of interest in engineering applications.

In the following, we assume that we are interested in the evaluation of N functionals, which we denote by $J_1, J_2, \dots, J_{N-1}$, and J_N. We already derived how to compute local error estimators for a single functional. It would be possible to compute the local error contribution of all N functionals separately, and add them up afterward. However, we would have to solve N adjoint problems in this case. Therefore, we follow the idea in [42, 41] to combine the goal functionals. To this end, we assume that a solution u of problem (2.1) and the chosen $\tilde{u} \in U$ belong to $\bigcap_{i=1}^N \mathcal{D}(J_i)$, where $\mathcal{D}(J_i)$ describes the domain of J_i.

Definition 5.1 (error-weighting function [29]). *Let $M \subseteq \mathbb{R}^N$. We say that $\mathfrak{E} : (\mathbb{R}_0^+)^N \times M \mapsto \mathbb{R}_0^+$ is an* error-weighting function *if $\mathfrak{E}(\cdot, m) \in \mathcal{C}^1((\mathbb{R}_0^+)^N, \mathbb{R}_0^+)$ is strictly monotonically increasing in each component and $\mathfrak{E}(0, m) = 0\ \forall m \in M$.*

Let us define $\vec{J} : \bigcap_{i=1}^N \mathcal{D}(J_i) \subseteq U \mapsto \mathbb{R}^N$ as $\vec{J}(v) := (J_1(v), J_2(v), \dots, J_N(v))\ \forall v \in \bigcap_{i=1}^N \mathcal{D}(J_i)$. Furthermore, we define the operation $|\cdot|_N : \mathbb{R}^N \mapsto (\mathbb{R}_0^+)^N$ as $|x|_N := (|x_1|, |x_2|, \dots, |x_N|)$ for $x \in \mathbb{R}^N$. Following [29], the error functional is given by

$$\tilde{J}_{\mathfrak{E}}(v) := \mathfrak{E}(|\vec{J}(u) - \vec{J}(v)|_N, \vec{J}(\tilde{u})) \qquad \forall v \in \bigcap_{i=1}^N \mathcal{D}(J_i).$$

Of course, the exact solution u is not known. Therefore, $\tilde{J}_{\mathfrak{E}}$ cannot be computed. As for the error estimate itself, we use the approximation $u_h^{(2)}$ in the enriched space instead of an exact solution u to approximate $\tilde{J}_{\mathfrak{E}}$ and $J_{\mathfrak{E}}$. This finally reads as follows:

$$J_{\mathfrak{E}}(v) := \mathfrak{E}(|\vec{J}(u_h^{(2)}) - \vec{J}(v)|_N, \vec{J}(\tilde{u})) \qquad \forall v \in \bigcap_{i=1}^N \mathcal{D}(J_i). \tag{5.1}$$

Proposition 5.1. *If Assumption 1 is fulfilled for $\tilde{u}_1$ and $\tilde{u}_2$, and if*

$$J_i(u_h^{(2)}) \ \notin\ [J_i(\tilde{u}_1), J_i(\tilde{u}_2)] \ \cup\ [J_i(\tilde{u}_2), J_i(\tilde{u}_1)]$$

$\forall J_i$, $i = 1, \dots, N$, then we avoid error cancellation, i.e., if $|J_i(u) - J_i(\tilde{u}_1)| \leq |J_i(u) - J_i(\tilde{u}_2)|\ \forall i \in \{1, \dots, N\}$, then $J_{\mathfrak{E}}(\tilde{u}_1) \leq J_{\mathfrak{E}}(\tilde{u}_2)$.

Proof. For $\tilde{J}_{\mathfrak{E}}$, it is clear that

$$\forall i \in \{1, \dots, N\} \qquad |J_i(u) - J_i(\tilde{u}_1)| \leq |J_i(u) - J_i(\tilde{u}_2)| \implies \tilde{J}_{\mathfrak{E}}(\tilde{u}_1) \leq \tilde{J}_{\mathfrak{E}}(\tilde{u}_2).$$

Indeed, for $|J_i(u) - J_i(\tilde{u}_1)| \leq |J_i(u) - J_i(\tilde{u}_2)|$, and due to the construction of the error weighting function $\mathfrak{E}$ (strictly monotonically increasing in each component), we do not obtain any error cancellation. However, since $J_i(u)$ is unknown, we work with the finer discrete solution $u_h^{(2)}$ rather than the exact solution u and show that

$$|J_i(u_h^{(2)}) - J_i(\tilde{u}_1)| \leq |J_i(u_h^{(2)}) - J_i(\tilde{u}_2)|$$

holds true. In other words,

$$|J_i(u) - J_i(\tilde{u}_1)| \leq |J_i(u) - J_i(\tilde{u}_2)|$$

and

$$J_i(u_h^{(2)}) \;\notin\; [J_i(\tilde{u}_1), J_i(\tilde{u}_2)] \;\cup\; [J_i(\tilde{u}_2), J_i(\tilde{u}_1)]$$

imply

$$|J_i(u_h^{(2)}) - J_i(\tilde{u}_1)| \leq |J_i(u_h^{(2)}) - J_i(\tilde{u}_2)|.$$

Without loss of generality, we assume that $J_i(u_h^{(2)}) < J_i(\tilde{u}_1)$ and $J_i(u_h^{(2)}) < J_i(\tilde{u}_2)$. From Assumption 1 and $J_i(u_h^{(2)}) \notin [J_i(\tilde{u}_1), J_i(\tilde{u}_2)] \cup [J_i(\tilde{u}_2), J_i(\tilde{u}_1)]$, we conclude that $J_i(u)$ does not belong to the union of the intervals $[J_i(\tilde{u}_1), J_i(\tilde{u}_2)]$ and $[J_i(\tilde{u}_2), J_i(\tilde{u}_1)]$. We now distinguish two cases. First, if $J_i(\tilde{u}_1) = J_i(\tilde{u}_2)$, the statement

$$|J_i(u_h^{(2)}) - J_i(\tilde{u}_1)| \leq |J_i(u_h^{(2)}) - J_i(\tilde{u}_2)|$$

follows immediately. In the second case, for $J_i(\tilde{u}_1) \neq J_i(\tilde{u}_2)$, Assumption 1 allows us to conclude that we have either

$$J_i(u_h^{(2)}) \leq J_i(u) < J_i(\tilde{u}_1) < J_i(\tilde{u}_2)$$

or

$$J_i(u) < J_i(u_h^{(2)}) < J_i(\tilde{u}_1) < J_i(\tilde{u}_2).$$

Both cases imply $|J_i(u_h^{(2)}) - J_i(\tilde{u}_1)| \leq |J_i(u_h^{(2)}) - J_i(\tilde{u}_2)|$, which concludes the proof. ∎

Remark 9. We notice that in [42, 41, 31], the functionals were combined as follows:

$$J_c(v) := \sum_{i=1}^{N} \frac{\omega_i \; \mathrm{sign}(J_i(u_h^{(2)}) - J_i(\tilde{u}))}{|J_i(\tilde{u})|} J_i(v) \quad \forall v \in \bigcap_{i=0}^{N} \mathcal{D}(J_i).$$

For the error weighting function $\mathfrak{E}(x, \vec{J}(\tilde{u})) := \sum_{i=1}^{N} \frac{\omega_i x_i}{|J_i(\tilde{u})|}$, which yields that the error functional $J_{\mathfrak{E}}$ coincides with $(-J_c)$ up to a constant [29], the condition

$$J_i(u_h^{(2)}) \;\notin\; [J_i(\tilde{u}_1), J_i(\tilde{u}_2)] \;\cup\; [J_i(\tilde{u}_2), J_i(\tilde{u}_1)]$$

is not required to avoid error cancellation.

6. Algorithms.

In this section, we describe the algorithmic realizations of our theoretical work. The spatial discretization is based on the finite element method. However, the algorithms presented below can be adapted to other discretization techniques as well.

6.1. Newton's algorithm.

Newton's method for solving the nonlinear variational problem (2.2) on refinement level l is stated in Algorithm 1. Below we identify $u_h^{l,k}$ with the corresponding vector with respect to the chosen basis when we compute $\|\delta u_h^{l,k}\|_{\ell_\infty}$. Furthermore for the following algorithm let $\varsigma_h^{l,k}$ be defined as

$$\varsigma_h^{l,k} := \frac{\|\delta u_h^{l,k-1}\|_{\ell_\infty}}{1 - (\|\delta u_h^{l,k-1}\|_{\ell_\infty} / \|\delta u_h^{l,k-2}\|_{\ell_\infty})^2},$$

leading to a stopping criteria which is motivated by [26].

Algorithm 1 Adaptive Newton algorithm for multiple goal functionals on level l.

1: Start with some initial guess $u_h^{l,0} \in U_h^l$, set $k=0$, and set $TOL_{Newton}^l > 0$.
2: **while** $\varsigma_h^{l,k} > TOL_{Newton}^l(\|u_h^{l,k}\|_{\ell_\infty} + \|\delta u_h^{l,k-1}\|_{\ell_\infty})$ or $\varsigma_h^{l,k} < 0$ **do**
3: Solve for $\delta u_h^{l,k}$,

$$\mathcal{A}'(u_h^{l,k})(\delta u_h^{l,k}, v_h) = -\mathcal{A}(u_h^{l,k})(v_h) \quad \forall v_h \in V_h^l.$$

4: Update : $u_h^{l,k+1} = u_h^{l,k} + \alpha \delta u_h^{l,k}$ for some good choice $\alpha \in (0,1]$.
5: $k = k+1$.

Remark 10. The arising linear systems are solved by using the direct solver UMFPACK [24].

Remark 11. In Algorithm 1, we choose $\|\delta u_h^{l,-2}\|_{\ell_\infty} := 1$, $\|\delta u_h^{l,-1}\|_{\ell_\infty} := 0.99$ and $TOL_{Newton}^l = 10^{-8}$. To compute α, we use the same line search method as described in [29].

6.2. Adaptive Newton algorithms for multiple goal functionals. In this section, we describe the key algorithm. The basic structure of the algorithm is similar to that presented in [29, 66] and [34]. In contrast to previous work, we replace the stopping criteria $|A(u_h^{l,k})(z_h^{l,k})| > 10^{-2}\eta_h^{l-1}$, which was used in [29], by $|(J_{\mathfrak{E}}^{(k)})'(\delta u_h^{l,k})| > 10^{-2}\eta_h^{l-1}$. However, this is possible only since we assume that the linear problem is solved exactly, and we replace the error estimator on the current level by that of the previous level.

Remark 12. In the algorithms developed in [66], the computation of the adjoint solution could not be avoided since it was also needed to compute the current discretization error estimator.

Remark 13. The last Newton update in Algorithm 2 is used only in the stopping criterion. Of course, one can use this update to perform a very last Newton update step for a final improvement of the solution.

Remark 14. We can also use Algorithm 2 for the enriched problem, replacing the stopping criterion $|(J_{\mathfrak{E}}^{(k)})'(\delta u_h^{l,k})| > 10^{-2}\eta_h^{l-1}$ by $|J_i'(\delta u_h^{l,k})| < TOL_i^l$. This stopping criterion can also be used for this algorithm, which makes Algorithm 3 more flexible.

6.3. The final algorithm. In this subsection, we formulate the overall algorithm starting with an initial mesh $\mathcal{T}_h^1$ and the corresponding finite element spaces V_h^1, U_h^1, $U_h^{1,(2)}$, and $V_h^{1,(2)}$, where $U_h^{1,(2)}$ and $V_h^{1,(2)}$ are the enriched finite element spaces. The refinement procedure creates a sequence of finer and finer meshes $\mathcal{T}_h^l$ leading to the corresponding finite element spaces V_h^l, U_h^l, $U_h^{l,(2)}$, and $V_h^{l,(2)}$ for $l = 2, 3, \ldots$.

As already explained above, we replace the estimated error $\eta_h^{l,(2)}$ by $\eta_h^{l-1,(2)}$ to avoid the evaluation of the error estimator and the computation of the adjoint solution in step 3 of Algorithm 2. Thus, η_h^{l-1} is not defined on the first level. Therefore, we set $\eta_h^0 := 10^{-8}$. This means that we perform more iterations on the coarsest level. However, solving on this level is very cheap.

Remark 15. The refinement procedure used in our numerical examples in step 7 of Algorithm 3 is based on the *fixed-rate strategy* described in [10] with $X = 0.1$ and $Y = 0.0$. This means we mark 10% of the total elements (rounded to the larger integer) for refinement with the largest error contribution.

Algorithm 2 Adaptive Newton algorithm for multiple goal functionals on level l.

1: Start with some initial guess $u_h^{l,0} \in U_h^l$ and $k = 0$.
2: Construct $(J_{\mathfrak{E}}^{(0)})'$ employing $u_h^{l,(2)}$ (obtained by (2.2) using Algorithm 1) and $u_h^{l,0}$
3: For $\delta u_h^{l,k}$, solve

$$\mathcal{A}'(u_h^{l,k})(\delta u_h^{l,k}, v_h) = -\mathcal{A}(u_h^{l,k})(v_h) \quad \forall v_h \in V_h^l.$$

4: **while** $|(J_{\mathfrak{E}}^{(k)})'(\delta u_h^{l,k})| > 10^{-2}\eta_h^{l-1}$ **do**
5: Update : $u_h^{l,k+1} = u_h^{l,k} + \alpha \delta u_h^{l,k}$ for some good choice $\alpha \in (0, 1]$.
6: $k = k + 1$.
7: For $\delta u_h^{l,k}$, solve

$$\mathcal{A}'(u_h^{l,k})(\delta u_h^{l,k}, v_h) = -\mathcal{A}(u_h^{l,k})(v_h) \quad \forall v_h \in V_h^l.$$

8: Construct $(J_{\mathfrak{E}}^{(k)})'$ constructed with $u_h^{l,(2)}$ and $u_h^{l,k}$

Algorithm 3 The final algorithm.

1: Start with some initial guess $u_h^{0,(2)}$,u_h^0, set $l = 1$, and set $TOL_{dis} > 0$.
2: Solve (2.2) for $u_h^{l,(2)}$ using Algorithm 1 with the initial guess $u_h^{l-1,(2)}$ on the discrete space $U_h^{l,(2)}$.
3: Solve (2.2) using Algorithm 2 with the initial guess u_h^{l-1} on the discrete spaces U_h^l.
4: Construct the combined functional $J_{\mathfrak{E}}$ as in (5.1).
5: Solve the adjoint problem (2.4) for $J_{\mathfrak{E}}$ on $V_h^{l,(2)}$ and V_h^l.
6: Construct the error estimator η_K by distributing η_i defined in (4.1) to the elements and adding the local remainder contributions $\eta_{\mathcal{R},K}^{(2)}$ defined in (4.4).
7: Mark elements with some refinement strategy.
8: Refine marked elements: $\mathcal{T}_h^l \mapsto \mathcal{T}_h^{l+1}$ and $l = l + 1$.
9: If $|\eta_h| < TOL_{dis}$ stop, else go to 2.

7. Numerical examples. In order to support our theoretical and algorithmic developments, some numerical tests are performed in this section. The first part is devoted to the regularized p-Laplace equation. In these tests, we also provide computational hints on the validity of the saturation assumptions (despite that, for the specific choices made, we cannot prove that the saturation assumptions hold true).

In the second part, we discuss the application to a (stationary) Navier–Stokes benchmark problem. Here we observe that the saturation assumption is not always fulfilled.

The implementation is based on the finite element library deal.II [6] and the extension of our previous implementation [31, 29]. In case of multiple goal functionals, we use the error weighting function $\mathfrak{E}(x, \vec{J}(\tilde{u})) := \sum_{i=1}^N x_i/|J_i(\tilde{u})|$ (for the definition we refer back to section 5). The computations are done on the cluster RADON1.[1]

7.1. Regularized *p*-Laplace. The first set of tests is based on a regularized p-Laplace equation with a very small regularization parameter $\varepsilon > 0$ and $p \in (1, \infty)$.

[1] https://www.ricam.oeaw.ac.at/hpc/overview/.

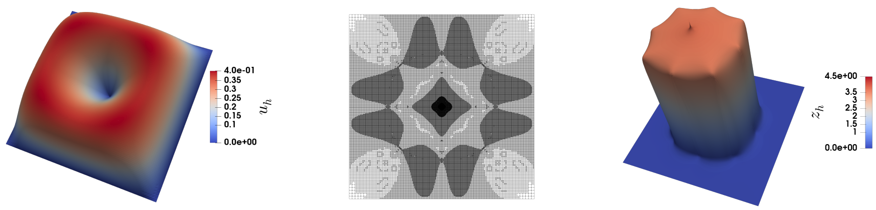

FIG. 2. *Example* 1a: *Approximation of the solution (left), the adjoint solution (right) on the mesh (middle) achieved on level $l = 31$ (144 785 DOFs).*

In the first test, we consider a problem with a nonsmooth analytical solution on the unit square. Here we investigate the behavior in the case of single goal functionals. In the second test, we investigate the behavior of multiple goal functionals on a more complicated domain. For the regularized p-Laplace equation, we use the same finite element discretizations as in our previous work [29], i.e., continuous bilinear elements for U_h and V_h and continuous bi-quadratic elements for the enriched spaces $U_h^{(2)}$ and $V_h^{(2)}$ in the 2D case.

7.1.1. A single goal functional (Example 1a). In the first set of computations, we consider the boundary value problem

$$-\operatorname{div}((\varepsilon^2 + |\nabla u|^2)^{\frac{p-2}{2}} \nabla u) = f \text{ in } \Omega \quad \text{and} \quad u = 0 \text{ on } \partial\Omega \tag{7.1}$$

with $p = 4$ and $\varepsilon = 10^{-10}$ and f such that $u(x, y) = \sqrt{x^2 + y^2}(x^2 - 1)(y^2 - 1)$ is the exact solution. The computational domain Ω is the unit square $(-1, 1) \times (-1, 1)$. As goal functional we consider

$$J(u) := u(0, 0) = 0.$$

This point is exactly where the singularity of the solution is, which is visualized in Figure 2 (left). Furthermore, there is a line singularity, where $\nabla u = 0$ leading to additional refinement on these lines and a high gradient of the adjoint solution z_h due to the small regularization parameter, which can be monitored at Figure 2 (middle, right).

Inspecting the error in our goal functional $u(0, 0)$ for uniform refinement shown in Figure 3, it turns out that we have a worse convergence rate than $\mathcal{O}(\text{DOFs}^{-\frac{1}{2}}) \approx \mathcal{O}(h)$. Adaptivity leads to a convergence rate of approximately $\mathcal{O}(\text{DOFs}^{-1})$, i.e., to reach the same accuracy as with more than 1,000,000, DOFs using uniform refinement, we need less than 10,000 DOFs.

Furthermore, we monitor that the influences of the remainder term and iteration error vanish during the refinement process, as expected. Specifically, the estimator part $|\eta_{\mathcal{R}}^{(2)}|$ shows a higher-order behavior as expected but has an influence on coarse meshes.

Moreover, in this numerical example, Assumptions 1 and 2 seem to be fulfilled even with the additional condition that $b_h \to 0$ and $b_{h,\gamma} \to 0$ on adaptive meshes, which we also observe in Figure 4 as well as in Table 1. On the other hand, we observe a completely different behavior on uniformly refined meshes in Figure 5. The effectivity indices are approximately $0.1 - 0.2$, i.e., our estimator determines the error better on adaptively refined meshes. In Theorem 3.7, we prove that the efficiency depends on the constant b_0 in the saturation assumption. We assume that, for this example, b_0 is closer to 1 in the case of uniform refinement, while, for adaptive refinement, we also

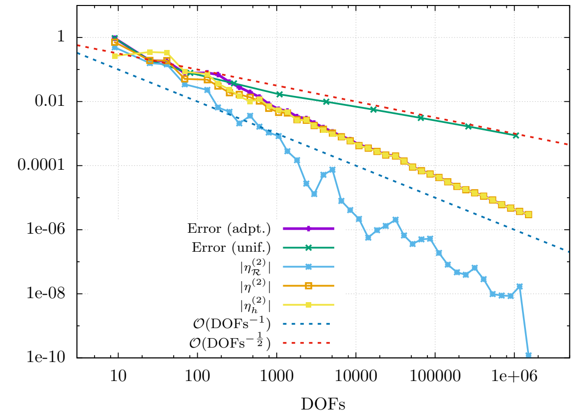

FIG. 3. *Example* 1a: *Error versus DOFs for $p = 4$, $\varepsilon = 10^{-10}$. Error (unif.) describes the error for uniform refinement in $J(u)$ and Error (adpt.) for adaptive refinement.*

TABLE 1

Example 1a: *Effectivity indices and errors for adaptive refinement. Here, l denotes the refinement level. Several intermediate levels are left out for the sake of a clearly arranged table.*

l	DOFs	I_{eff}	$I_{eff,\gamma}$	$\lvert\eta^{(2)}\rvert$	$\lvert\eta_h^{(2)}\rvert$	$\lvert J(u) - J(u_h)\rvert$
1	9	0.753	0.237	7.17E-01	2.26E-01	9.52E-01
2	25	1.007	1.836	1.93E-01	3.51E-01	1.91E-01
5	133	0.608	0.910	4.80E-02	7.18E-02	7.89E-02
10	605	0.745	0.858	1.04E-02	1.20E-02	1.39E-02
15	2 365	0.882	0.877	2.61E-03	2.59E-03	2.95E-03
20	8 481	0.923	0.917	6.00E-04	5.95E-04	6.49E-04
25	31 649	0.984	0.973	2.00E-04	1.98E-04	2.03E-04
30	111 793	0.995	0.992	4.27E-05	4.26E-05	4.29E-05
35	410 201	0.999	0.996	1.12E-05	1.12E-05	1.12E-05
39	1 166 237	1.000	1.004	3.74E-06	3.76E-06	3.74E-06
40	1 513 865	1.000	1.000	2.96E-06	2.96E-06	2.96E-06

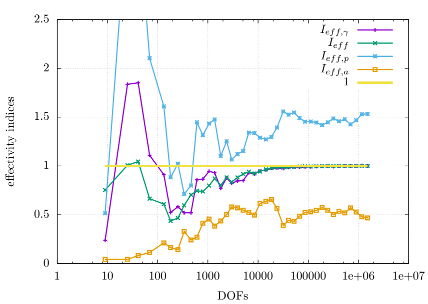

FIG. 4. *Example* 1a: *Effectivity indices for adaptive refinement.*

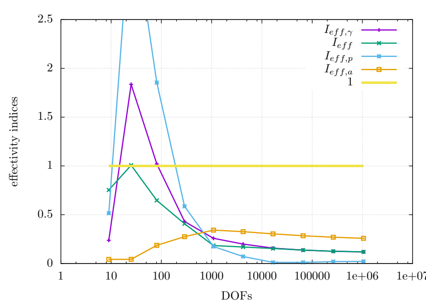

FIG. 5. *Example* 1a: *Effectivity indices for uniform refinement.*

recover parts of the optimal convergence rate for the enriched space, and, therefore, we obtain $b_h \to 0$ and $b_{h,\gamma} \to 0$.

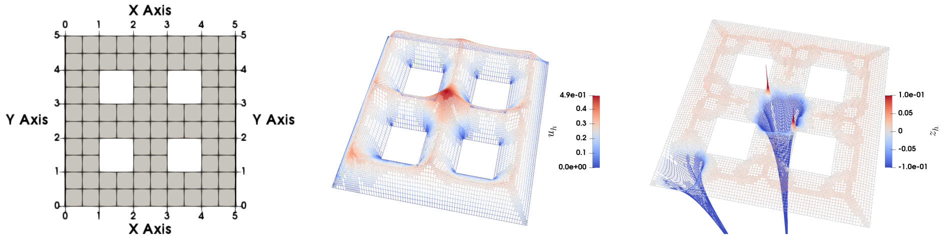

Fig. 6. *Example* 1b: *Initial mesh (left), the primal solution (middle), and adjoint solution (right) on the mesh achieved on level $l = 22$ (24 532 DOFs).*

7.1.2. Multiple goal functionals (Example 1b). In the second example, we again consider the nonlinear boundary value problem (7.1), but with a different right-hand side and a different computational domain Ω. Specifically, we choose $f \equiv 1$. The computational domain is sketched in Figure 6 (left).

This example already was considered in our previous work [29] with the same parameters $p = 4$ and $\varepsilon = 10^{-10}$. Furthermore, we consider the same functionals of interest which are given by

$$\begin{aligned}
J_1(u) &:= (1 + u(2.9, 2.1))(1 + u(2.1, 2.9)),\\
J_2(u) &:= \left(\int_\Omega u(x,y) - u(2.5, 2.5)\ \mathrm{d}(x,y)\right)^2,\\
J_3(u) &:= \int_{(2,3)\times(2,3)} u(x,y)\ \mathrm{d}(x,y),\\
J_4(u) &:= u(0.6, 0.6),
\end{aligned}$$

with the same approximations as in [29], where a reference solution on a fine grid (8 uniform refinements, Q_c^2 elements, 22,038,525 DOFs) was computed on the cluster RADON1.[2] Our findings are shown in Figure 7 (effectivity indices), Figure 8 (error reduction uniform mesh refinment), Figure 9 (different error parts), and Figure 10 (error reduction with adaptive refinement).

7.2. A 2D stationary Navier–Stokes benchmark problem with muliple goal functionals. This example serves as a counterexample for the saturation assumption. We consider the steady state incompressible Navier–Stokes benchmark problem 2D-1 proposed in [70]; see also [17, 14, 18, 39]. The computational domain Ω is given by $(0, 2.2) \times (0, H) \setminus B$ with $H = 0.41$ and B is given by the ball with center $(0.2, 0.2)$ and radius 0.05. For a sketch of the geometry, we refer the reader to [70].

7.2.1. Equations and setup. The governing equations are given by the following boundary value problem: Find $\mathbf{u} := (u, p) \in [H^1(\Omega)]^2 \times L^2(\Omega)$ such that

$$\begin{aligned}
-\nu\Delta u + (u\cdot\nabla)u - \nabla p &= 0 && \text{in } \Omega,\\
\nabla\cdot u &= 0 && \text{in } \Omega,\\
u &= 0 && \text{on } \Gamma_{\text{no-slip}},\\
u &= \hat{u} && \text{on } \Gamma_{\text{inflow}},\\
\nu\frac{\partial u}{\partial \vec{n}} - p\cdot\vec{n} &= 0 && \text{on } \Gamma_{\text{outflow}}
\end{aligned} \tag{7.2}$$

[2]https://www.ricam.oeaw.ac.at/hpc/overview/.

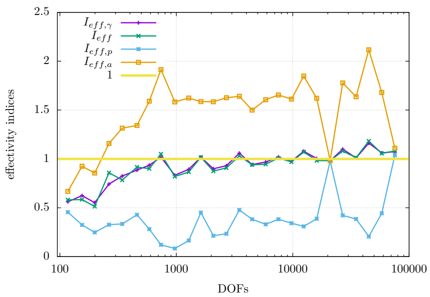

FIG. 7. *Example* 1b: *Effectivity indices for adaptive refinement for multiple goals.*

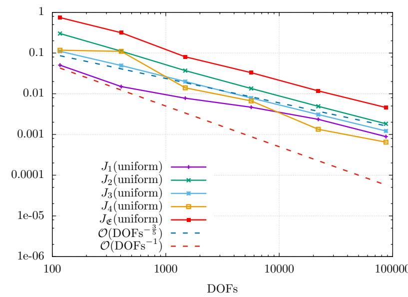

FIG. 8. *Example* 1b: *Error reduction for the single functionals using uniform refinement.*

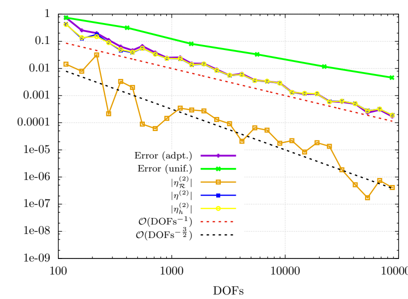

FIG. 9. *Example* 1b: *Comparison of the different error parts and the error in the uniform and adaptive case for the combined functional* $J_{\mathfrak{E}}$.

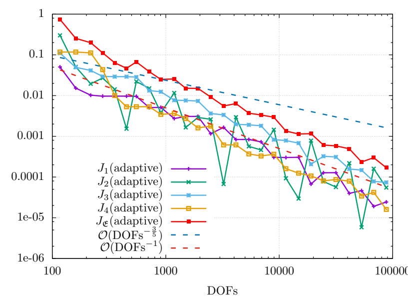

FIG. 10. *Example* 1b: *Error reduction for the single functionals using adaptive refinement.*

with the viscosity $\nu = 10^{-3}$. The boundaries are given by

$$\begin{aligned}
\Gamma_{\text{inflow}} &:= \{x = 0\} \cap \partial\Omega,\\
\Gamma_{\text{outflow}} &:= (\{x = 2.2\} \cap \partial\Omega) \setminus \partial(\{x = 2.2\} \cap \partial\Omega),\\
\Gamma_{\text{no-slip}} &:= \overline{\partial\Omega \setminus (\Gamma_{\text{inflow}} \cup \Gamma_{\text{outflow}})},
\end{aligned}$$

The function $\hat{u}$, describing the inflow, is defined by $\hat{u}(x, y) := (3w(y)/10, 0)$ with $w(y) = 4y(H - y)/H^2$. We notice that the pressure is uniquely determined due to the do-nothing condition prescribed on Γ_{outflow}; see [43].

7.2.2. Goal functionals. As in the original benchmark proposal [70], we consider the following quantities of interest:

$$\begin{aligned}
\Delta p(\mathbf{u}) &:= p(X_1) - p(X_2),\\
c_{drag}(\mathbf{u}) &:= C \int_{\partial B} \left[\nu \frac{\partial u}{\partial \vec{n}} - p\vec{n}\right] \cdot \vec{e}_1 \ \mathrm{d}s_{(x,y,z)},\\
c_{lift}(\mathbf{u}) &:= C \int_{\partial B} \left[\nu \frac{\partial u}{\partial \vec{n}} - p\vec{n}\right] \cdot \vec{e}_2 \ \mathrm{d}s_{(x,y,z)}
\end{aligned}$$

with $C = 500$, $X_1 = (0.15, 0.2)$, $X_2 = (0.25, 0.2)$, $\vec{e}_1 := (1, 0)$, $\vec{e}_2 := (0, 1)$, and $\vec{n}$ denotes the outer normal vector.

These three functionals are controlled simultaneously (i.e., with our multiple goal functional framework) using the practical error estimator (3.3). We notice that goal

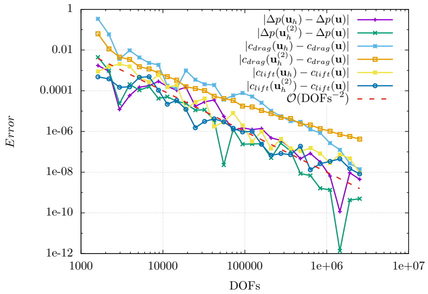

FIG. 11. *Example* 2: *Absolute errors for the finite element space and the enriched space.*

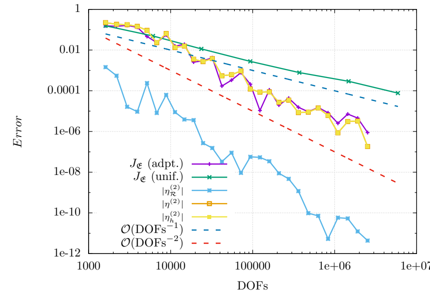

FIG. 12. *Example* 2: *Error in* $J_{\mathfrak{E}}$ *for uniform and adaptive refinements, and the estimated error and its parts in case of adaptive refinement.*

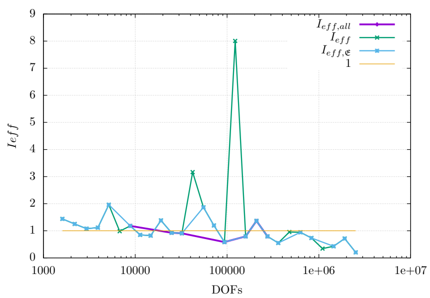

FIG. 13. *Example* 2: *Effectivity index: restricted to the refinements where the saturation assumption for all three functionals is fulfilled* ($I_{eff,all}$), *restricted to the refinements where the saturation assumption for* $J_{\mathfrak{E}}$ *is fulfilled* ($I_{eff,\mathfrak{E}}$), *without restriction* (I_{eff}).

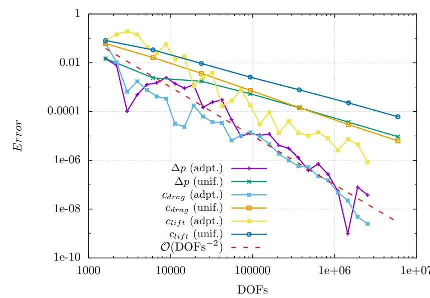

FIG. 14. *Example* 2: *Relative errors for the adaptive and uniform refinements.*

oriented adaptivity for single goal functionals for this problem was already applied in [17, 14, 18, 39].

Furthermore, for the finite element spaces, we choose $U_h := V_h := [Q_2^C]^2 \times Q_1^C$, and for the enriched spaces $U_h^{(2)} := V_h^{(2)} := [Q_4^C]^2 \times Q_2^C$, i.e., continuous bi-quadratic elements for the pressure p fourth-order polynomials for the velocity u. Finally, we notice that our error estimator does not estimate the error arising from the approximation of the ball.

7.2.3. Results and discussion. The reference values, which are taken from the featflow webpage[3] and [55], are given by

$$\begin{aligned} \Delta p(\mathbf{u}) &= 0.11752016697, \\ c_{drag}(\mathbf{u}) &= 5.57953523384, \\ c_{lift}(\mathbf{u}) &= 0.010618948146. \end{aligned}$$

Our findings are shown in Figures 11, 12, 13, 14, 15, and in Table 2.

[3]http://www.featflow.de/en/benchmarks/cfdbenchmarking/flow/dfg_benchmark1_re20.html.

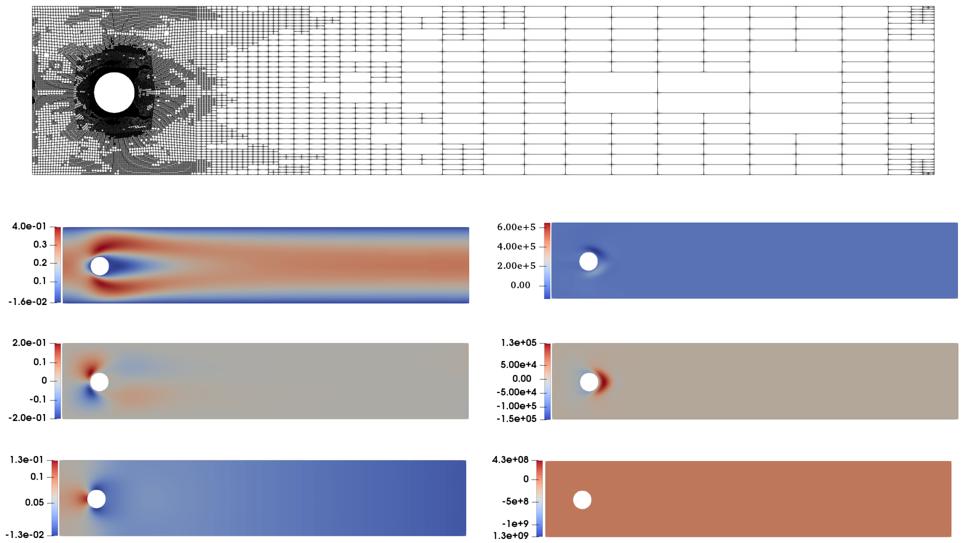

FIG. 15. *Example 2: Mesh (top) and solutions (u_x, u_y, and p on the left from top to bottom and their adjoint counterparts on the right) after 23 refinement step for all three goal functionals simultaneously controlled.*

First, in Figure 11, the errors of the standard finite element space and the enriched finite element space are plotted. We observe that, in some cases, the error using the enriched space is larger. However, this violates both saturation assumptions, i.e., Assumptions 1 and 2 posed in section 3.

Next, in Figure 12, the combined goal functional and its estimator are shown for uniform and adaptive mesh refinement, respectively. Here, we observe nearly perfect agreement of the true error and the estimator yielding thus an effectivity index close to one. Moreover, the error of the remainder term $|\eta_{\mathcal{R}}^{(2)}|$ is several orders of magnitude smaller. Thus, it can be neglected (which is actually often done in the literature).

In Figure 13, a more quantitative behavior of the effectivity indices is displayed. In particular, we observe steps where the saturation assumption is violated. We can deduce that if the saturation assumption holds true for all functionals, it is also fulfilled for the combined functional, but not vice versa. Furthermore, we monitor that the effectivity indices are better on levels where the restrictions hold. Nevertheless, Figure 12 demonstrates that even though the saturation assumption is not fulfilled, we have a higher-order behavior in the remainder term. Then, in Figure 14 the relative errors for adaptive and uniform refinement are compared. Here our results indicate that the errors converge with a higher order when using adaptive mesh refinement. To obtain a similar accuracy as we have for 5,909,120 DOFs in the case of uniform refinement, 159,651 DOFs are required. The resulting mesh at refinement step 23 and the corresponding solution plots of the primal and adjoint solutions are plotted in Figure 15. Finally, in Table 2, we summarize our most important findings. The values for the effectivity indices are provided as well as the bounds for the saturation assumption introduced in section 3. These values highlight again in which refinement steps the saturation assumption is violated.

TABLE 2

Example 2: Errors, effectivity indices, and bounds for the saturation assumption, where $E := J_{\mathfrak{E}}(\boldsymbol{u}) - J_{\mathfrak{E}}(\boldsymbol{u}_h)$ *and* c_d *denotes* c_{drag} *and* c_l *denotes* c_{lift}.

l	$\lvert\mathcal{T}_h\rvert$	DOFs	E	$\eta^{(2)}$	I_{eff}	$I_{eff,\gamma}$	$b_{\Delta p,h}$	$b_{c_d,h}$	$b_{c_l,h}$
1	160	1 610	1.56E-01	2.25E-01	1.43	1.44	2.54	0.18	0.55
2	211	2 189	1.48E-01	1.85E-01	1.26	1.25	1.07	0.19	0.24
3	277	2 946	1.63E-01	1.76E-01	1.08	1.08	1.93	1.23	0.07
4	361	3 919	1.32E-01	1.47E-01	1.12	1.12	3.58	0.36	0.10
5	472	5 153	4.66E-02	9.14E-02	1.99	1.96	0.71	0.35	1.01
6	616	6 770	2.34E-02	2.30E-02	0.98	0.98	0.89	0.51	1.77
7	802	8 824	5.56E-02	6.56E-02	1.18	1.18	0.15	0.40	0.18
8	1 045	11 302	1.57E-02	1.33E-02	0.84	0.85	0.31	2.84	0.15
9	1 360	14 716	1.92E-02	1.58E-02	0.82	0.82	0.29	2.54	0.18
10	1 771	19 072	2.57E-03	3.55E-03	1.38	1.38	0.16	0.16	1.03
11	2 305	24 870	2.93E-03	2.71E-03	0.93	0.93	0.64	0.37	0.05
12	2 998	32 230	4.20E-03	3.80E-03	0.91	0.91	0.41	0.49	0.08
13	3 901	42 193	1.71E-04	5.43E-04	3.17	3.17	0.10	0.28	2.39
14	5 116	55 307	3.32E-04	6.19E-04	1.87	1.87	0.00	1.13	1.01
15	6 658	72 033	7.78E-04	9.30E-04	1.20	1.20	1.12	0.57	0.17
16	8 692	93 723	2.10E-04	1.23E-04	0.58	0.58	0.16	0.23	0.49
17	11 338	122 671	1.07E-05	8.59E-05	8.00	8.01	0.20	0.31	3.12
18	14 827	159 651	1.11E-04	8.78E-05	0.80	0.79	0.18	0.42	0.23
19	19 456	209 144	1.98E-05	2.70E-05	1.37	1.37	0.10	0.73	0.46
20	25 552	275 400	4.35E-05	3.45E-05	0.79	0.79	0.72	0.88	0.20
21	33 430	361 400	1.55E-05	8.52E-06	0.55	0.55	0.73	1.35	0.50
22	44 314	477 308	9.30E-06	8.87E-06	0.95	0.95	0.18	0.80	1.73
23	58 084	630 242	1.51E-05	1.43E-05	0.95	0.94	0.08	1.65	0.09
24	76 879	830 637	8.31E-06	6.10E-06	0.73	0.73	0.05	1.62	0.31
25	101 128	1 095 812	2.53E-06	8.66E-07	0.34	0.34	0.21	3.84	1.21
26	133 132	1 445 379	7.19E-06	3.09E-06	0.43	0.43	0.01	5.64	0.59
27	175 723	1 910 027	4.57E-06	3.27E-06	0.71	0.71	0.05	21.26	0.31
28	231 385	2 519 211	8.89E-07	1.81E-07	0.21	0.20	0.11	30.19	0.92

8. Conclusions. In this work, we further investigated and developed a posteriori error estimation and mesh adaptivity using the dual-weighted residual method for treating multiple goal functionals. This framework includes both nonlinear PDEs and nonlinear goal functionals and estimation of the discretization error and the nonlinear iteration error. The latter can be used as a stopping criterion for the nonlinear solver, e.g., for the Newton solver that is used in our numerical experiments. Using a saturation assumption, we could establish the efficiency of the error estimator. These theoretical findings give insight into the influence of the choice of the enriched space that is used to approximate the unknown exact solution in the error estimator. Our developments are substantiated with carefully designed numerical tests. Moreover, our studies also include investigations of the influence of the remainder term to the error estimator. Summarizing, we have designed a well-tested framework for the regularized

p-Laplacian and a 2D Navier–Stokes benchmark problem that will be extended in near-future work to some of the promised (stationary) multiphysics applications mentioned in the introduction.

Acknowledgments. The authors would like to thank D. Jodlbauer, A. Schafelner, and W. Zulehner for helpful discussions. Furthermore, we thank both reviewers for their useful comments for improving the paper.

REFERENCES

[1] B. Achchab, S. Achchab, and A. Agouzal, *Some remarks about the hierarchical a posteriori error estimate*, Numer. Methods Partial Differential Equations, 20 (2004), pp. 919–932.

[2] A. Agouzal, *On the saturation assumption and hierarchical a posteriori error estimator*, Comput. Methods Appl. Math., 2 (2002), pp. 125–131.

[3] M. Ainsworth and J. T. Oden, *A posteriori error estimation in finite element analysis*, Comput. Methods Appl. Mech. Engrg., 142 (1997), pp. 1–88.

[4] M. Ainsworth and R. Rankin, *Guaranteed computable bounds on quantities of interest in finite element computations*, Internat. J. Numer. Methods Engrg., 89 (2012), pp. 1605–1634.

[5] J. Alvarez-Aramberri, D. Pardo, and H. Barucq, *Inversion of magnetotelluric measurements using multigoal oriented hp-adaptivity*, Procedia Computer Science, 18 (2013), pp. 1564–1573.

[6] G. Alzetta, D. Arndt, W. Bangerth, V. Boddu, B. Brands, D. Davydov, R. Gassmöller, T. Heister, L. Heltai, K. Kormann, M. Kronbichler, M. Maier, J.-P. Pelteret, B. Turcksin, and D. Wells, *The `deal.II` library, version* 9.0, J. Numer. Math., 26 (2018), pp. 173–183.

[7] L. Angermann, *Balanced a posteriori error estimates for finite-volume type discretizations of convection-dominated elliptic problems*, Computing, 55 (1995), pp. 305–323.

[8] T. Apel, A.-M. Sändig, and J. R. Whiteman, *Graded mesh refinement and error estimates for finite element solutions of elliptic boundary value problems in non-smooth domains*, Math. Methods Appl. Sci., 19 (1996), pp. 63–85.

[9] I. Babuška and W. C. Rheinboldt, *A-posteriori error estimates for the finite element method*, Internat. J. Numer. Methods Engrg., 12 (1978), pp. 1597–1615.

[10] W. Bangerth and R. Rannacher, *Adaptive Finite Element Methods for Differential Equations*, Birkhäuser Verlag, Boston, 2003.

[11] R. E. Bank, A. Parsania, and S. Sauter, *Saturation estimates for hp-finite element methods*, Comput. Vis. Sci., 16 (2013), pp. 195–217.

[12] R. E. Bank and R. K. Smith, *A posteriori error estimates based on hierarchical bases*, SIAM J. Numer. Anal., 30 (1993), pp. 921–935.

[13] R. E. Bank and A. Weiser, *Some a posteriori error estimators for elliptic partial differential equations*, Math. Comp., 44 (1985), pp. 283–301.

[14] R. Becker, *Weighted Error Estimators for the Incompressible Navier-Stokes Equations*, Technical report RR-3458, INRIA, 1998.

[15] R. Becker, R. Estecahandy, and D. Trujillo, *Weighted marking for goal-oriented adaptive finite element methods*, SIAM J. Numer. Anal., 49 (2011), pp. 2451–2469.

[16] R. Becker, C. Johnson, and R. Rannacher, *Adaptive error control for multigrid finite element methods*, Computing, 55 (1995), pp. 271–288.

[17] R. Becker and R. Rannacher, *Weighted a posteriori error control in FE methods*, in Proceedings of ENUMATH'97, H. G. Bock, ed., World Scientific, Singapore, 1995.

[18] R. Becker and R. Rannacher, *A general concept of adaptivity in finite element methods with applications to problems in fluid and structural mechanics*, in Grid Generation and Adaptive Algorithms, M. W. Bern, J. E. Flaherty, and M. Luskin, eds., Springer, New York, 1998, pp. 51–75.

[19] R. Becker and R. Rannacher, *An optimal control approach to a posteriori error estimation in finite element methods*, Acta Numer., 10 (2001), pp. 1–102.

[20] F. A. Bornemann, B. Erdmann, and R. Kornhuber, *A posteriori error estimates for elliptic problems in two and three space dimensions*, SIAM J. Numer. Anal., 33 (1996), pp. 1188–1204.

[21] M. Braack and A. Ern, *A posteriori control of modeling errors and discretization errors*, Multiscale Model. Simul., 1 (2003), pp. 221–238.

[22] M. P. Bruchhäuser, K. Schwegler, and M. Bause, *Numerical study of goal-oriented error control for stabilized finite element methods*, in Advanced Finite Element Methods with Applications: Selected Papers from the 30th Chemnitz Finite Element Symposium 2017, Springer, New York, 2019, pp. 85–106.

[23] C. Carstensen, D. Gallistl, and J. Gedicke, *Justification of the saturation assumption*, Numer. Math., 134 (2016), pp. 1–25.

[24] T. A. Davis, *Algorithm* 832: *Umfpack v*4.3*—an unsymmetric-pattern multifrontal method*, ACM Trans. Math. Software, 30 (2004), pp. 196–199.

[25] A. De Rossi, *Saturation Assumption and Finite Element Method for a One-Dimensional Model*, RGMIA Research Report Collection 5, 2002, 13.

[26] P. Deuflhard, *Newton Methods for Nonlinear Problems*, Springer Ser. Comput. Math. 35, Springer, New York, 2011.

[27] L. Diening and M. Růžička, *Interpolation operators in Orlicz-Sobolev spaces*, Numer. Math., 107 (2007), pp. 107–129.

[28] W. Dörfler and R. H. Nochetto, *Small data oscillation implies the saturation assumption*, Numer. Math., 91 (2002), pp. 1–12.

[29] B. Endtmayer, U. Langer, and T. Wick, *Multigoal-oriented error estimates for non-linear problems*, J. Numer. Math., to appear, https://doi.org/10.1515/jnma-2018-0038.

[30] B. Endtmayer, U. Langer, and T. Wick, *Multiple goal-oriented error estimates applied to* 3*d non-linear problems*, PAMM, 18 (2018), e201800048.

[31] B. Endtmayer and T. Wick, *A partition-of-unity dual-weighted residual approach for multi-objective goal functional error estimation applied to elliptic problems*, Comput. Methods Appl. Math., 17 (2017), pp. 575–599.

[32] C. Erath, G. Gantner, and D. Praetorius, *Optimal Convergence Behavior of Adaptive FEM Driven by Simple* $(h - h/2)$*-Type Error Estimators*, arXiv.1805.00715 [math.NA], 2018.

[33] K. Eriksson, D. Estep, P. Hansbo, and C. Johnson, *Introduction to adaptive methods for differential equations*, Acta Numer., 4 (1995), pp. 105–158.

[34] A. Ern and M. Vohralík, *Adaptive inexact Newton methods with a posteriori stopping criteria for nonlinear diffusion PDEs*, SIAM J. Sci. Comput., 35 (2013), pp. A1761–A1791.

[35] M. Feischl, D. Praetorius, and K. G. van der Zee, *An abstract analysis of optimal goal-oriented adaptivity*, SIAM J. Numer. Anal., 54 (2016), pp. 1423–1448.

[36] S. Ferraz-Leite, C. Ortner, and D. Praetorius, *Convergence of simple adaptive Galerkin schemes based on* $h - h/2$ *error estimators*, Numer. Math., 116 (2010), pp. 291–316.

[37] M. Giles and Niles A. Pierce, *Analysis of Adjoint Error Correction for Superconvergent Functional Estimates*, Oxford University Computing Laboratory Report NA 01/14, 2001.

[38] M. B. Giles and E. Süli, *Adjoint methods for PDEs: A posteriori error analysis and post-processing by duality*, Acta Numer., 11 (2002), pp. 145–236.

[39] C. Goll, T. Wick, and W. Wollner, *DOpElib: Differential equations and optimization environment; A goal oriented software library for solving PDEs and optimization problems with PDEs*, Arch. Numer. Softw., 5 (2017), pp. 1–14.

[40] W. Han, *A Posteriori Error Analysis Via Duality Theory: With Applications in Modeling and Numerical Approximations*, Adv. Mech. Math., Springer, New York, 2005.

[41] R. Hartmann, *Multitarget error estimation and adaptivity in aerodynamic flow simulations*, SIAM J. Sci. Comput., 31 (2008), pp. 708–731.

[42] R. Hartmann and P. Houston, *Goal-oriented a posteriori error estimation for multiple target functionals*, in Hyperbolic Problems: Theory, Numerics, Applications, Springer, New York, 2003, pp. 579–588.

[43] J. G. Heywood, R. Rannacher, and S. Turek, *Artificial boundaries and flux and pressure conditions for the incompressible Navier-Stokes equations*, Internat. J. Numer. Methods Fluids, 22 (1996), pp. 325–352.

[44] A. Hirn, *Finite element approximation of singular power-law systems*, Math. Comp., 82 (2013), pp. 1247–1268.

[45] M. Holst and S. Pollock, *Convergence of goal-oriented adaptive finite element methods for nonsymmetric problems*, Numer. Methods Partial Differential Equations, 32 (2016), pp. 479–509.

[46] M. Holst, S. Pollock, and Y. Zhu, *Convergence of goal-oriented adaptive finite element methods for semilinear problems*, Comput. Vis. Sci., 17 (2015), pp. 43–63.

[47] K. Kergrene, S. Prudhomme, L. Chamoin, and M. Laforest, *A new goal-oriented formulation of the finite element method*, Comput. Methods Appl. Mech. Engrg., 327 (2017), pp. 256–276.

[48] H. Kim and S.-G. Kim, *Saturation assumptions for a 1d convection-diffusion model*, Korean J. Math., 22 (2014), pp. 599–609.

[49] S. K. Kleiss and S. K. Tomar, *Guaranteed and sharp a posteriori error estimates in isogeometric analysis*, Comput. Math. Appl., 70 (2015), pp. 167–190.

[50] U. Köcher, M. P. Bruchhäuser, and M. Bause, *Efficient and scalable data structures and algorithms for goal-oriented adaptivity of space–time FEM codes*, SoftwareX, 10 (2019), 100239.

[51] P. Ladevèze, F. Pled, and L. Chamoin, *New bounding techniques for goal-oriented error estimation applied to linear problems*, Internat. J. Numer. Methods Engrg., 93 (2013), pp. 1345–1380.

[52] U. Langer, S. Matculevich, and S. Repin, *Guaranteed Error Control Bounds for the Stabilised Space-Time IgA Approximations to Parabolic Problem*, arXiv:1712.06017 [math.NA], 2017.

[53] D. Meidner, R. Rannacher, and J. Vihharev, *Goal-oriented error control of the iterative solution of finite element equations*, J. Numer. Math., 17 (2009), pp. 143–172.

[54] K.-S. Moon, E. von Schwerin, A. Szepessy, and R. Tempone, *Convergence rates for an adaptive dual weighted residual finite element algorithm*, BIT, 46 (2006), pp. 367–407.

[55] G. Nabh, *On High Order Methods for the Stationary Incompressible Navier-Stokes Equations*, Ph.D. thesis, University of Heidelberg, 1998.

[56] P. Neittaanmäki and S. Repin, *Reliable Methods for Computer Simulation: Error Control and Posteriori Estimates*, Elsevier, Amsterdam, 2004.

[57] R. H. Nochetto, A. Schmidt, K. G. Siebert, and A. Veeser, *Pointwise a posteriori error estimates for monotone semi-linear equations*, Numer. Math., 104 (2006), pp. 515–538.

[58] R. H. Nochetto, A. Veeser, and M. Verani, *A safeguarded dual weighted residual method*, IMA J. Numer. Anal., 29 (2009), pp. 126–140.

[59] D. Pardo, *Multigoal-oriented adaptivity for hp-finite element methods*, Procedia Computer Science, 1 (2010), pp. 1953–1961.

[60] S.-H. Park, K.-C. Kwon, and S.-K. Youn, *A posteriori error estimates and an adaptive scheme of least-squares meshfree method*, Internat. J. Numer. Methods Engrg., 58 (2003), pp. 1213–1250.

[61] N. A. Pierce and M. B. Giles, *Adjoint recovery of superconvergent functionals from PDE approximations*, SIAM Rev., 42 (2000), pp. 247–264.

[62] N. A. Pierce and M. B. Giles, *Adjoint and defect error bounding and correction for functional estimates*, J. Comput. Phys., 200 (2004), pp. 769–794.

[63] S. Prudhomme and J. T. Oden, *On goal-oriented error estimation for elliptic problems: Application to the control of pointwise errors*, Comput. Methods Appl. Mech. Engrg., 176 (1999), pp. 313–331.

[64] S. Prudhomme, J. T. Oden, T. Westermann, J. Bass, and M. E. Botkin, *Practical methods for a posteriori error estimation in engineering applications*, Internat. J. Numer. Methods Engrg., 56 (2003), pp. 1193–1224.

[65] R. Rannacher and F.-T. Suttmeier, *A feed-back approach to error control in finite element methods: Application to linear elasticity*, Comput. Mech., 19 (1997), pp. 434–446.

[66] R. Rannacher and J. Vihharev, *Adaptive finite element analysis of nonlinear problems: Balancing of discretization and iteration errors*, J. Numer. Math., 21 (2013), pp. 23–61.

[67] R. Rannacher, A. Westenberger, and W. Wollner, *Adaptive finite element solution of eigenvalue problems: Balancing of discretization and iteration error*, J. Numer. Math., 18 (2010), pp. 303–327.

[68] S. Repin, *A posteriori estimates for partial differential equations*, Radon Ser. Comput. Appl. Math. 4, De Gruyter, Berlin, 2008.

[69] T. Richter and T. Wick, *Variational localizations of the dual weighted residual estimator*, J. Comput. Appl. Math., 279 (2015), pp. 192–208.

[70] M. Schäfer, S. Turek, F. Durst, E. Krause, and R. Rannacher, *Benchmark computations of laminar flow around a cylinder*, in Flow Simulation with High-Performance Computers II, Notes Numer. Fluid Mech, 48, Springer, New York, 1996, pp. 547–566.

[71] M. Sharbatdar and C. Ollivier-Gooch, *Adjoint-based functional correction for unstructured mesh finite volume methods*, J. Sci. Comput., 76 (2018), pp. 1–23.

[72] P. Stolfo, A. Rademacher, and A. Schröder, *Dual Weighted Residual Error Estimation for the Finite Cell Method*, Ergeb. Instit. Angew. Mathe. 576, TU Dortmund, 2017.

[73] I. Toulopoulos and T. Wick, *Numerical methods for power-law diffusion problems*, SIAM J. Sci. Comput., 39 (2017), pp. A681–A710.

[74] E. H. van Brummelen, S. Zhuk, and G. J. van Zwieten, *Worst-case multi-objective error estimation and adaptivity*, Comput. Methods Appl. Mech. Engrg., 313 (2017), pp. 723–743.

[75] R. Verfürth, *A Review of A Posteriori Error Estimation and Adaptive Mesh-Refinement Techniques*, Wiley-Teubner, New York, 1996.
[76] S. Weisser and T. Wick, *The dual-weighted residual estimator realized on polygonal meshes*, Comput. Methods Appl. Math., 18 (2018), pp. 753–776.
[77] O. C. Zienkiewicz, D. W. Kelly, J. Gago, and I. Babuška, *Hierarchical finite element approaches, error estimates and adaptive refinement*, in The Mathematics of Finite Elements and Applications, IV (Uxbridge, 1981), Academic Press, New York, 1982, pp. 313–346.